Journal of Pharmaceutical and Biomedical Analysis 163 (2019) 180–187

Contents lists available at ScienceDirect

Journal of Pharmaceutical and Biomedical Analysis

journal homepage: www.elsevier.com/locate/jpba

Ultrasensitive and reusable electrochemical aptasensor for detection of tryptophan using of $[Fe(bpy)_3](p\text{-}CH_3C_6H_4SO_2)_2$ as an electroactive indicator

Ayemeh Bagheri Hashkavayi[a,b], Jahan Bakhsh Raoof[a,*]

[a] Electroanalytical Chemistry Research Laboratory, Department of Analytical Chemistry, Faculty of Chemistry, University of Mazandaran, Babolsar, Iran
[b] Department of Chemical Industry, Faculty of Alzahra, Bushehr Branch, Technical and Vocational University (TVU), Bushehr, Iran

ARTICLE INFO

Article history:
Received 5 August 2018
Received in revised form
24 September 2018
Accepted 2 October 2018
Available online 3 October 2018

Keywords:
Aptamer
Tryptophan
Reusable aptasensor
Carbon screen-printed electrode

ABSTRACT

In this paper, we report the application of a reusable electrochemical aptasensor for detection of tryptophan by using $[Fe(bpy)_3](p\text{-}CH_3C_6H_4SO_2)_2$ as an electroactive indicator and based on the target-compelled aptamer displacement. The aptasensor fabricated by self-assembling the thiolated probe on the surface of graphite screen-printed electrode modified with gold nanoparticles/multiwalled carbon nanotubes and chitosan nanocomposite (AuNPs/MWCNTs-Chit/SPE). Afterward, Trp aptamer (Apt) immobilized on the modified electrode surface through hybridization. In the absence of Trp, a sharp peak of $[Fe(bpy)_3](p\text{-}CH_3C_6H_4\ SO_2)_2$ can be observed in differential pulse voltammetry (DPV) study. The introduction of Trp led to the formation of aptamer-Trp complex and dissociation of the aptamer from the DNA-Apt duplex on the electrode surface into the solution and decreases the peak current intensity of electroactive indicator. This is because, $[Fe(bpy)_3](p\text{-}CH_3C_6H_4SO_2)_2$ tends to bind to the two strands DNA. Therefore, the peak current of $[Fe(bpy)_3](p\text{-}CH_3C_6H_4\ SO_2)_2$ linearly decreased with increasing the concentration of Trp over a range of 3.0 nM- 100 μM. The detection limit (3 σ) was 1.0 nM. In addition, we examined the selectivity of the constructed biosensor for tyrosine, histidine, arginine, lysine, valine and methionine that belonged to the amino acid family.

The obtained results showed that the fabricated sensor had a good selectivity for Trp against the other examined amino acids. Also, the potential applicability of the aptasensor was investigated by detecting the Trp in a complex media such as human blood plasma spiked with Trp.

1. Introduction

Diagnosis and quantitative determination of amino acids play an essential role in biomedical studies, pharmaceutical industries and clinical applications [1,2]. Tryptophan (Trp) is a required amino acid in humans and animals for brain functions and a precursor for some hormones and vitamins) serotonin, melatonin and niacin) [3]. The concentration of TRP in human blood is very important, because it is a probable cause of many diseases [4]. Therefore, development of a highly sensitive and selective technique for recognition and determination of TRP is so important.

In recent years, affinity biosensors have attracted much consideration and there has been great interest in the development of biosensors that use aptamers as the biorecognition element (aptasensors) [5]. Aptamers are artificial single-stranded oligonucleotides, which are selected from random RNA or DNA libraries for the first time in 1990 by SELEX[1] [6,7]. Since their discovery, aptamers have attracted considerable attention in biosensor development [8–11].

Numerous aptasensor have been developed using different analytical methods, including optical [12], electrochemical techniques [13,14], fluorimetry [15], quartz crystal microbalance (QCM) [16] and colorimetry [17]. Among various aptamer-based biosensors, electrochemical aptasensors have received much attention due to distinct benefits such as good excellent sensitivity and selectivity for detection of various targets, portability, low production cost and fast response [5].

A considerably improved performance for aptasensors can be obtained by modifying the electrode surface with different nano

* Corresponding author.
E-mail address: j.raoof@umz.ac.ir (J.B. Raoof).

[1] systematic evolution of ligands by exponential enrichment

https://doi.org/10.1016/j.jpba.2018.10.006
0731-7085/

particles [18–20]. Among the various nanomaterials, a carbon nanotube (CNT) is highly regarded due to exclusive properties such as high mechanical resistance, conducting, good biocompatibility and high specific surface area [21,22]. Furthermore, we used chitosan, a biocompatible and nontoxic polymer, for the preparation of stable nanocomposite. As a result, through noncovalent binding, multiwalled CNTs (MWCNTs) can be uniformly dispersed in a chitosan film and leads to a homogeneous black solution [23]. Then, gold nanoparticles (AuNPs) were electrodeposited on the MWCNTs- Chit modified screen printed electrode (SPE) for attachment of the thiolated probe. Also, in this work, $[Fe(bpy)_3](p\text{-}CH_3C_6H_4SO_2)_2$ was used as an electrochemical indicator and a reporter for the detection events. Transition metal complexes and pyridine derivatives have important biological activities as the part of some vitamins, enzymes, proteins and also have been widely applied in cancer therapy [24]. Commonly transition metal complexes can interact with nucleic acid by intercalation or groove-binding.

In the present study, we report a simple, label-free and reusable electrochemical aptasensor for the determination of Trp based on the target-compelled strand displacement mechanism from DNA/apt duplex to apt/target complex. The fabrication of reusable Trp aptasensor was based on the self-assembly of thiolated DNA (part of the complementary strand of aptamer) onto the AuNps/MWCNTs-Chit/SPE and then, immobilization of the aptamer on the surface via its hybridization with the thiolated DNA. Upon Trp binding, aptamer was taken off from the electrode due to the formation of a complex between the aptamer and Trp, and part complementary strands remains at the modified electrode surface. Thus with this technique, a reusable sensing system will be provided [25]. As mentioned above, transition metal complexes tend to interact with nucleic acid by intercalation, so with dissociation of the Trp/aptamer complex from the electrode surface, the peak current of $[Fe(bpy)_3](p\text{-}CH_3C_6H_4SO_2)_2$ decreased.

The main advantages and novelties of this work are: a) making a reusable sensor for detection and determination of Trp; b) construction of AuNps/MWCNTs -Chit/SPE with large specific surface area and also high conductivity; c) using $[Fe(bpy)_3](p\text{-}CH_3C_6H_4SO_2)_2$ as an electroactive indicator for determination of Trp and d) $[Fe(bpy)_3](p\text{-}CH_3C_6H_4SO_2)_2$/DNA-Apt/AuNps/MWCNTs-Chit/SPE was used for the first time to detect Trp, which shows a high sensitivity and specificity.

2. Materials and methods

2.1. Reagents and instruments

Trp aptamer and partly complementary DNA strand with 5'-thiol modification was purified with HPLC and obtained from Bioneer Co. (South Korea). The sequence of the selected aptamer for Trp and partly complementary strand DNA was as follows [26]:

Aptamer sequence: 5≠AGCACGTTGGTTAGGTCAGGTTT-GGGTTTCGTGC-3′.

DNA strand: 5′-SH-$(CH_2)_6$-GCACGAAACCCAAACCTG-3′.

All chemicals were of analytical grade and supplied from Aldrich or Merck Company. A 0.1 mM stock solution of aptamer was prepared by 0.05 M Tris-HCl, 1.0 mM EDTA (Tris-EDTA buffer, pH 8.0) and afterwards the prepared solution was kept at −20 °C. All solutions were prepared using ultrapure water.

Graphite screen-printed electrodes (GSPEs), consisted of the carbon working electrode, carbon counter electrode and silver pseudo reference electrode were bought from Florence, Italy.

Autolab PGstut 30 electrochemical analysis system controlled by GPES 4.9 and FRA software (Eco Chemie Netherlands) was used for all voltammetry and electrochemical impedance spectrometry (EIS) measurements. Also in each step of electrode modification, scanning electron microscopy images were obtained by Mira 3-XMU Field Emission SEM (FESEM).

2.2. Fabrication of the electrochemical Trp aptasensor

For the preparation of MWCNT-Chit nano composite, Chit (5.0 mg) was dissolved in 1.0 mL 1% acetic acid. Then, MWNTs (2.0 mg) was dissolved in prepared Chit solution and sonicated until a homogeneous mixture was obtained [27]. After the preparation of nanocomposite, the surface of the working electrode was modified with 7.0 μL of nano composite and allowed to dry at room temperature. Then, the synthesis of AuNPs was done by chronoamperometry at -0.23 V for 300 s in a solution containing 0.5 mM $HAuCl_4$ for the formation of gold nanoparticles on the surface of MWCNT-Chit/SPE. Subsequently, 8.0 μL of 2.0 μM thiolated DNA solution was placed on the AuNps/MWCNT-Chit/SPE for 6.0 h at room temperature. In the next step, 8.0 μL of 2.0 μM 34-bases Trp aptamer was immobilized on the surface of the prepared electrode through DNA hybridization reaction at room temperature for construction of DNA-Apt/AuNps/MWCNTs-Chit/SPE. After 100 min, 8.0 μL of (5 μM) $[Fe(bpy)_3](p\text{-}CH_3C_6H_4SO_2)_2$ was added onto the modified electrode surface for 20 min. After these processes, for determination of Trp, 8.0 μL of Trp solutions with different concentrations was dropped onto the modified electrode surface for 45 min. After each step, the surface of modified electrode was rinsed with double distilled water. At last, the peak current of $[Fe(bpy)_3](p\text{-}CH_3C_6H_4\ SO_2)_2$ was used to evaluate the Trp concentration. Scheme 1 illustrates the step by step fabrication procedure and the sensing mechanism of aptasensor.

3. Results

3.1. Optimization of effective parameters on aptasensor response

We optimized some of the experimental parameters such as hybridization and incubation time of the aptasensor for the analysis of the Trp. The effect of the hybridization time of DNA on the response of the aptasensor was optimized by EIS method. Fig. S1A shows the dependence of the R_{ct} to the hybridization time of the DNA. As seen, R_{ct} of the aptasensor obviously increased with increasing the hybridization time from 10 to 100 min and then starts to level off. Therefore, the optimum hybridization time between DNA and aptamer was found to be 100 min.

Furthermore, the effect of Trp incubation time on the response of the fabricated aptasensor was studied from 0 to 60 min (Fig. S1B). The interaction time includes both the interaction time of the Trp with the aptamer and the departure time of the aptamer-Trp complex from the electrode surface. As shown in Fig. S1B, with increasing the interaction time from 5 min to 45 min, R_{ct} decreased and reaches a minimum at 45 min but no significant change in R_{ct} was observed over 45 min. Thus, according to the obtained results, 45 min was chosen as the optimal incubation time. After 45 min hybridization, the sensing interface was approximately regenerated and can be reused.

3.2. Morphology study of the modified electrode

The morphology of modified SPE was investigated by FE-SEM images at each step. Fig. 1 (A–C) represents the FE-SEM images of the bare SPE, MWCNT-Chit/SPE and AuNPs/ MWCNT-Chit/SPE. As can be seen, Fig. 1B shows the forming of homogeneous and spaghetti-like porous MWCNT- Chit nanocomposites on the surface of the SPE. The obtained nanocomposite has good practicality, because of the high specific surface area and porous structure of the nanocomposite. After electrodeposition, the gold nanoparticles with sizes ranging from 21 nm to 28 nm were well distributed and

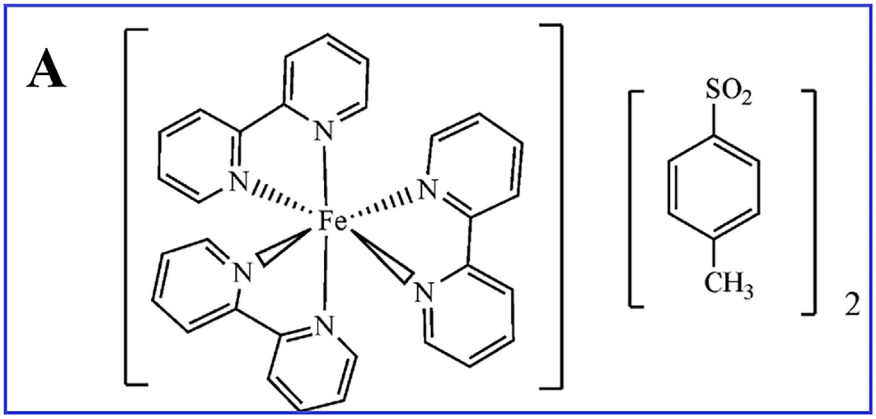

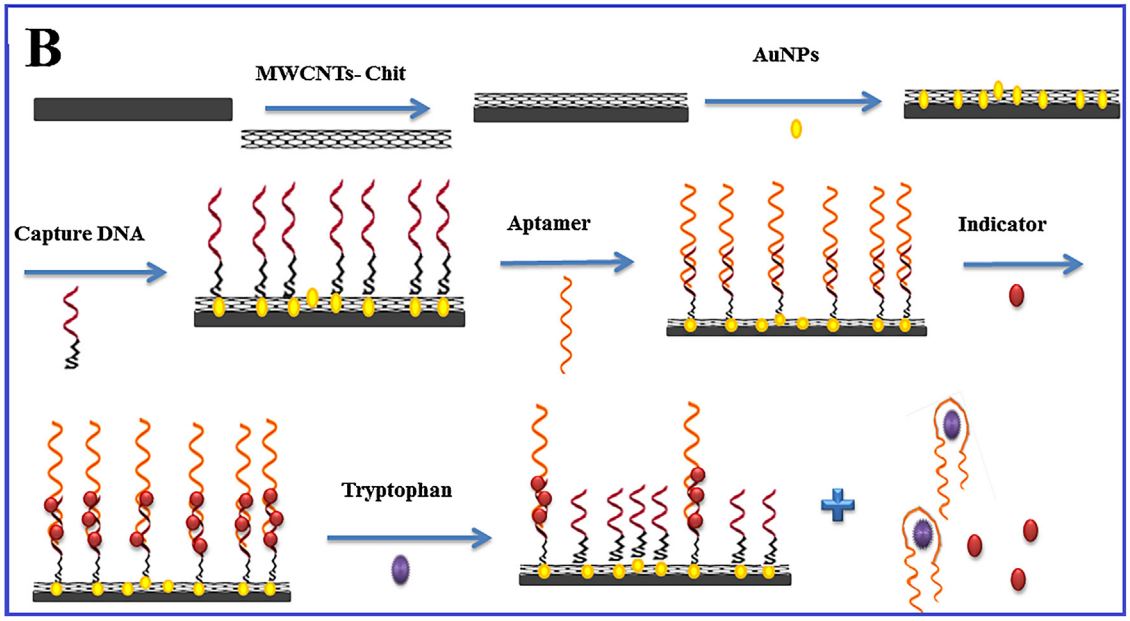

Scheme 1. (A) Chemical structure of the hemin, (B) Schematic representation of the construction of reusable electrochemical aptasensor for detection of Trp.

tightly attached on the modified electrode surface by linking to the hydroxyl and amino groups of the chitosan (Fig. 1C). This causes to improve the signal and also to strong binding of the DNA to the AuNPs/ MWCNT-Chit/SPE surface.

3.3. Electrochemical characterization of aptasensor

Electrochemical methods such as CV and EIS were widely used to affirm the changes in the fabrication process of the biosensors. Fig. 2A presents the cyclic voltammograms of 0.01 M Fe $(CN)_6^{3-/4-}$ at different steps of aptasensor preparation. The SPE electrode was first modified with MWCNTs- Chit (curve b), the peak currents of $[Fe(CN)6]^{3-/4-}$ on MWCNTs-Chit/SPE was higher than at bare SPE (curve a) and the ΔE_p value at the surface of MWCNTs-Chit/SPE decrease obviously compared with the bare SPE. The results show that MWCNTs-Chit can increase the electron transfer speed and effective surface area.

In the next step, electrodeposition of AuNPs on the MWCNTs-Chit/SPE, increased the peaks current intensity and the electrochemical reversibility of $[Fe\ (CN)_6]^{3-/4-}$ redox couple, which indicates that the immobilized AuNPs can improved the conductivity and also effective surface area of the modified electrode (curve c). After the immobilization of thiol-terminated DNA, the peaks current intensity of $Fe(CN)_6^{3-/4-}$ redox couple decreased (line d) with an increase in the peak-to-peak separation potential. This phenomenon can be attributed to the negative charges phosphate groups of the immobilized DNA on the surface of AuNPs/MWCNTs-Chit/SPE repelled the $[Fe(CN)_6]^{3-/4-}$ anions and confirmed the successful immobilization of the thiolated DNA on the surface of the prepared modified electrode. Also, after hybridization of aptamer with ssDNA on the modified electrode surface, further decrease of peaks current intensity and increase of ΔE_p of $[Fe\ (CN)_6]^{3-/4-}$ was observed (curve e).

Finally, after incubation with Trp (0.8 μM) for 45 min, redox peak currents of $[Fe(CN)_6]^{3-/4-}$ increased compared to the curve (e) and reached to the curve (d). This was ascribed to the fact that the formation of Trp/aptamer complex instead of aptamer-DNA and dissociation of the Trp/aptamer from the electrode surface. As a result, it can be concluded that a reusable sensor has been obtained. Also, the different stages of aptasensor preparation were followed using the EIS technique in the presence of the $[Fe(CN)_6]^{3-/4-}$ redox couple (Fig. 2B). The obtained results are in good accordance with the results from CV experiments. Thus, the results obtained from CV and EIS confirmed the successful fabrication of the aptasensor according to Scheme 1. After one time use of the prepared sensor we rinsed the modified

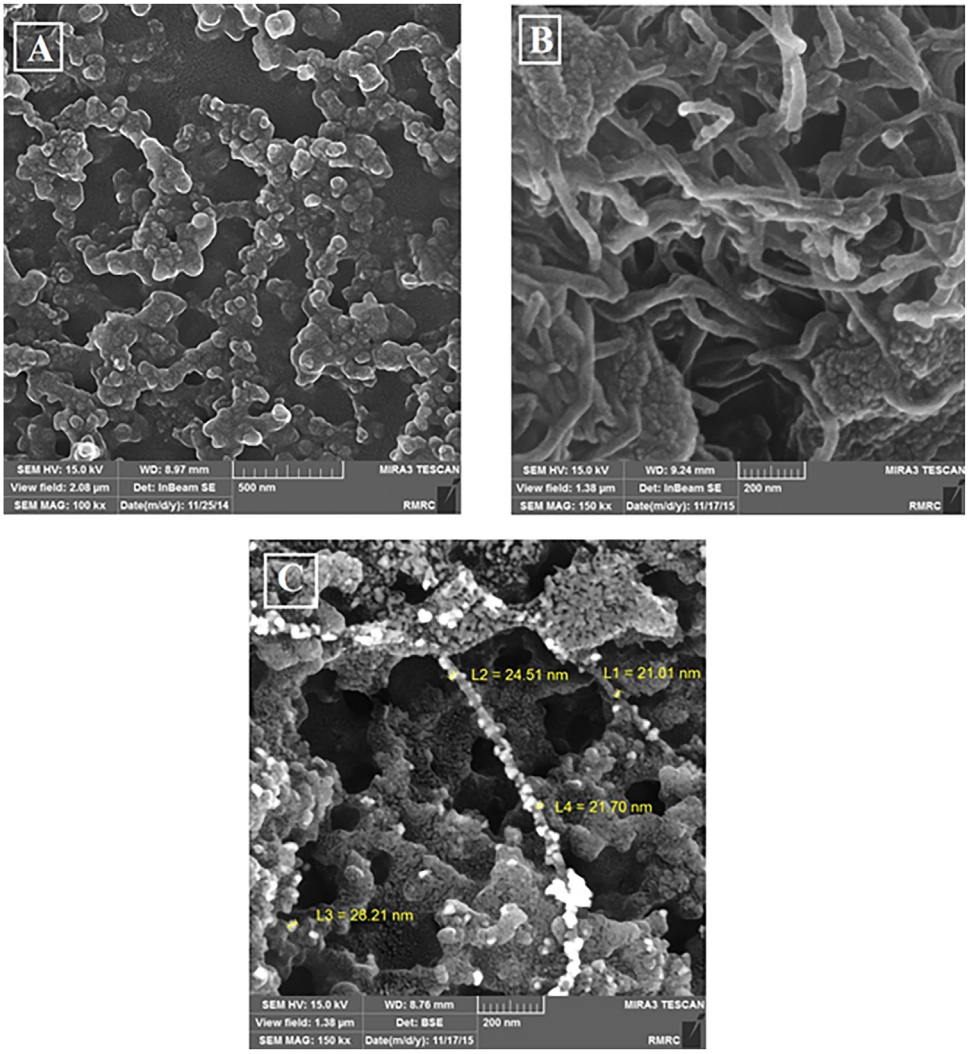

Fig. 1. Represents the FE-SEM images of the bare SPE (A), MWCNT-Chit/SPE (B) and AuNPs/ MWCNT-Chit/SPE(C).

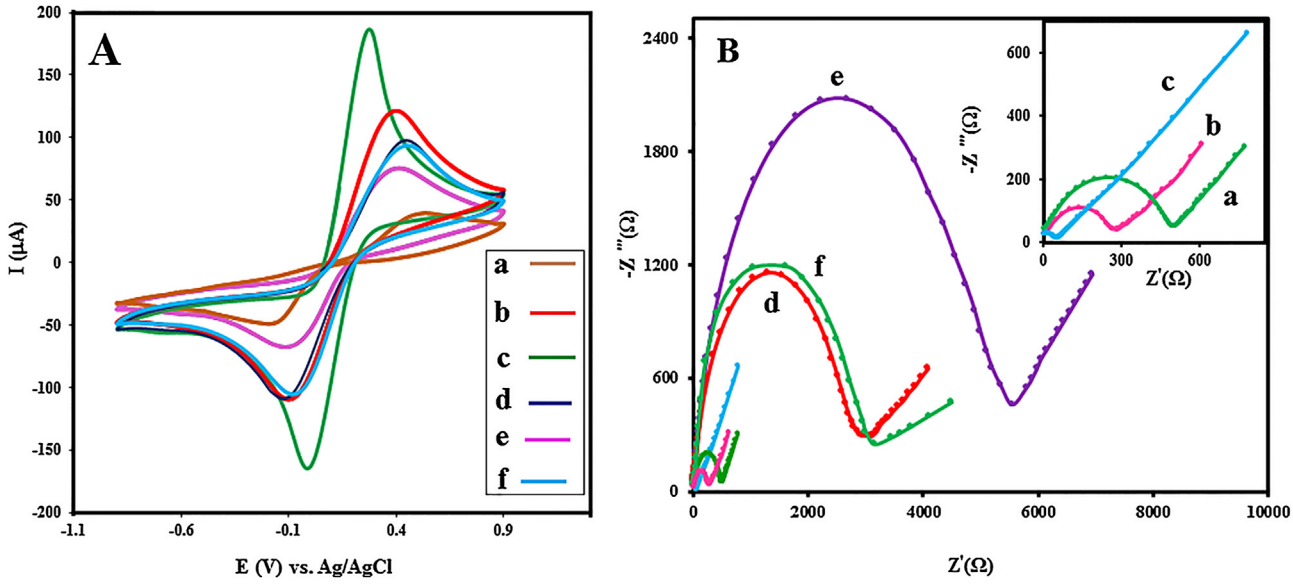

Fig. 2. (A) Cyclic voltammograms and (B) Nyquist plots of different modification steps of aptasensor: (a) bare SPE, (b) MWCNTs-Chit/SPE, (c) AuNPs/MWCNTs-Chit/SPE, (d) DNA/AuNPs/MWCNTs-Chit/SPE, (e) Apt/DNA/AuNPs/MWCNTs-Chit/SPE and (f) Trp/Apt/DNA/AuNPs/MWCNTs-Chit/SPE in 0.1 M PBS (pH 7. 0) containing 0.01 M $K_3[Fe(CN)_6]/K_4[Fe(CN)_6]$ (1:1) and 100 mM KCl. The insert show the electrical equivalent circuit of presented Nyquist plots of Fig. 2B.

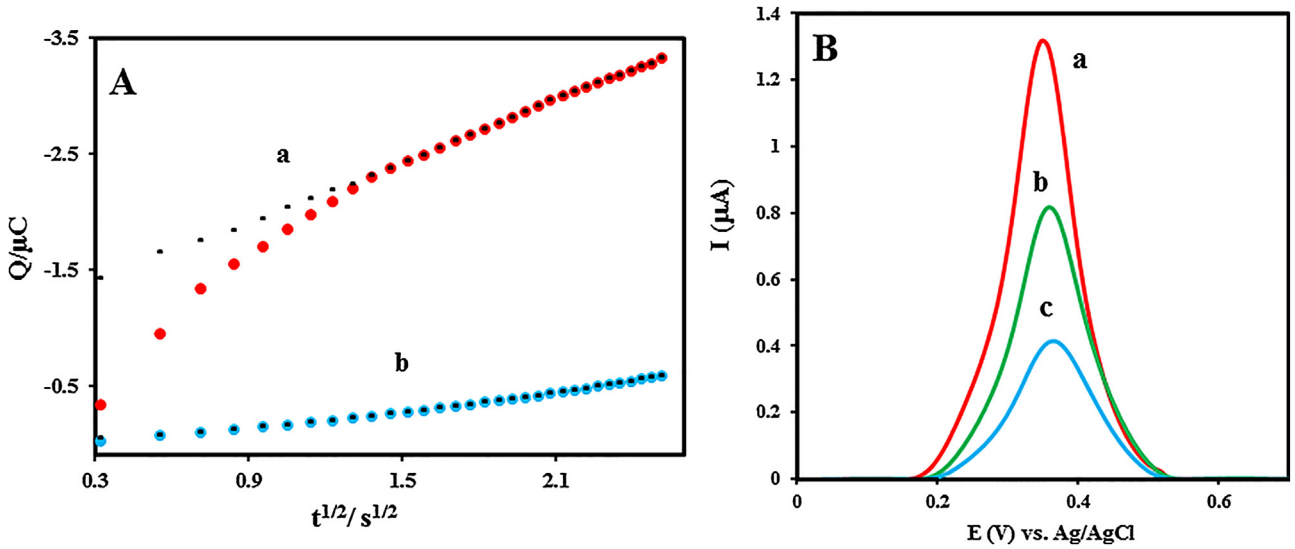

Fig. 3. (A) Chronocoloumetric curves at Apt/DNA/AuNps/MWCNTs-Chit/SPE in a solution of a) 200 μM ruthenium hexa-amine and 0.05 M potassium chloride (b) 0.05 M potassium chloride.
(B) DPV signals of (a) Ind/Apt/DNA/AuNPs/MWCNTs-Chit/SPE (b) Ind/Apt/DNA/AuNPs/ MWCNTs-Chit/SPE after incubation with 0.06 μM Trp, and (c) Ind/Apt/DNA/AuNPs/MWCNTs-Chit/SPE after incubation with 0.8 μM Trp in 0.1 M PBS (pH 7. 0).

electrode surface with double distilled water, then, for construction of DNA-Apt/AuNps/MWCNTs-Chit/SPE 7.0 μL (0.8 μM) of Trp aptamer solution was placed on the modified SPE for 100 min at room temperature. After hybridization, we examined the modified electrode surface using the EIS technique. The results were approximately similar to which obtained in Fig. 2B. Results showed that the measuring interface was almost entirely rebuilt and could be reused. The reusability of the fabricated sensor was investigated for the detection of Trp (0.8 μM), after 6 times using the sensor, the RSD of 2.3% has been achieved.

3.4. Quantitation of surface density of immobilized aptamer

The coverage of immobilized aptamer on the surface of AuNPs/MWCNTs-Chit/SPE was estimated by chronocoloumetric measurements and based on the electrostatic interaction of Apt and $[Ru(NH3)_6]^{3+}$. Measurements were performed at the AuNPs/MWCNTs-Chit/SPE in the absence and presence of 50.0 μM of the $[Ru(NH_3)_6]^{3+}$ (RuHex). Aptamer surface density computed using the following relationship [28]:

$$\Gamma = (Q/nFA)(z/m)N_A \quad (1)$$

Where Q(C) is the charge from the reduction of absorbed RuHex, calculated from the difference in chronocoloumetric intercepts in the presence and absence of RuHex, n is the number of electrons per molecule for reduction, F is the Faraday constant (C/equiv), A is the effective surface area of the electrode (cm^2), m is the number of bases in the aptamer, z is the number of electrons involved in the reduction of Ru (III) to Ru(II) and N_A Avogadro's number. For measuring the effective surface areas of the AuNPs/MWCNTs-Chit/SPE, the chronoamperogram of 0.5 mM $K_3Fe(CN)_6$ (redox probe) was recorded and the electroactive surface areas were calculated pursuant to Cottrell equation [29]:

$$i = nFAC * D^{1/2}/t^{1/2}\Pi^{1/2} \quad (2)$$

Where n is the number of electron transfers, D is the diffusion coefficient for redox probe (7.6×10^{-6} cm^2 s^{-1}), C* is the concentration of $K_3[Fe(CN)_6]$. The effective surface area was obtained as 1.3 cm^2 from the slope of Cottrell plot ($i\text{-}t^{-1/2}$) (Fig. S2). Finally, according to Fig. 3A, surface density of aptamers on AuNPs/MWCNTs-Chit/SPE has been obtained equal to 5.25×10^{17} molecule/cm^2.

3.5. Diagnosis principle of Trp aptasensor

Fig. 3 B shows the DPV signal of $[Fe(bpy)_3](p{-}CH_3C_6H_4SO_2)_2$ (Ind)[2] for the Apt-DNA/AuNPs/MWCNTs-Chit/SPE in the absence (curve a) and presence of Trp (curve b and curve c) in 0.1 M PBS (pH 7.0). Fig. 3B, curve a, shows the DPV signal for the Ind/Apt-DNA/AuNPs/MWCNTs-Chit/SPE. A peak was observed at 0.35 V in 0.1 M PBS (pH 7.0), showing the ability of the $[Fe(bpy)_3](p\text{-}CH_3C_6H_4SO_2)_2$ to bind to the double strand DNA (dsDNA). Since generally the transition metal complexes can interact with dsDNA by intercalation and groove-binding mode, after incubation with 0.06 μM (curve b) and 0.8 μM Trp (curve c), the peak current for the $[Fe(bpy)_3](p\text{-}CH_3C_6H_4SO_2)_2$ decreased in comparison with the curve a. The interaction between Trp and aptamer leading to the conformational changes of the aptamer, dissociation of the aptamer from the electrode surface and releasing the $[Fe(bpy)_3](p\text{-}CH_3C_6H_4SO_2)_2$, while the DNA stays connected to the electrode surface.

4. Discussion

4.1. Linear dynamic range and detection limit

The differential pulse voltammograms of the $[Fe(bpy)_3](p\text{-}CH_3C_6H_4SO_2)_2$ were recorded on the surface of Apt-DNA/AuNPs/MWCNTs-Chit/SPE after incubation with different concentrations of Trp. As shown in Fig. 4A, the peak current of $[Fe(bpy)_3](p\text{-}CH_3C_6H_4SO_2)_2$ decreased with the increasing of the concentration of Trp over the range of 0.003–100 μM. This means that the increasing of peak current of $[Fe(bpy)_3](p\text{-}CH_3C_6H_4SO_2)_2$ is due to the specific interaction between aptamer and Trp. In the other words, after the interaction of aptamer with the Trp, aptamer was desorbed from the surface of modified electrode and thus decrease the amount of $[Fe(bpy)_3](p\text{-}CH_3C_6H_4SO_2)_2$ on the

[2] Indicator

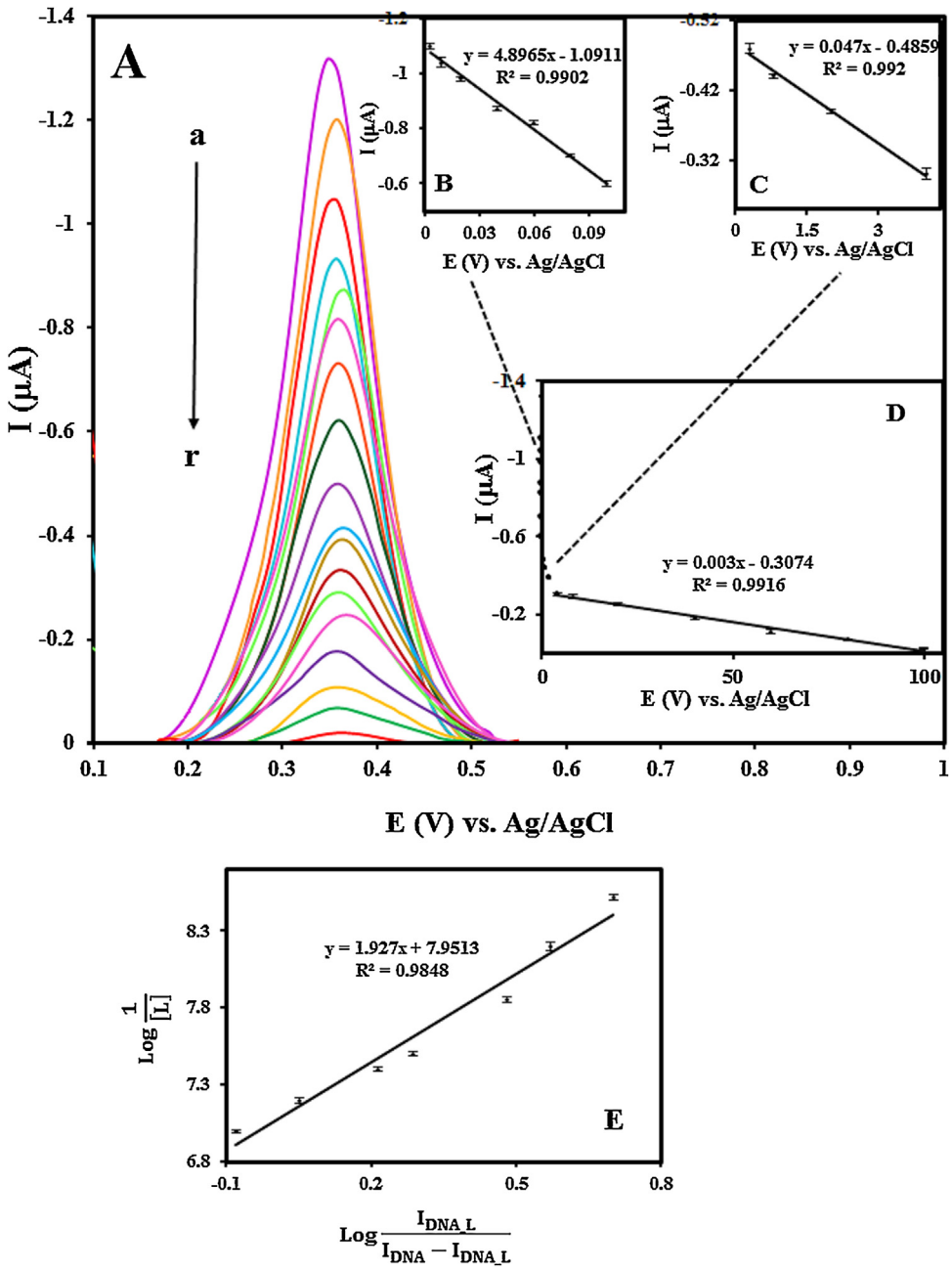

Fig. 4. (A) DPV signals of Ind/Apt/DNA/AuNPs/MWCNTs-Chit/SPE after incubation with different Trp concentrations in the absence (a) and presence of different concentrations of Trp: (b) 0.003, (c) 0.009, (d) 0.02, (e) 0.04, (f) 0.06, (g) 0.08, (h) 0.1, (i) 0.3, (j) 0.8, (k) 2.0, (l) 4.0, (m) 8.0, (n) 20 (o) 40, (p) 60, (q) 80 and (r) 100 μM in 0.1 M PBS (pH 7.0). B, C and D are the calibration plots of I_p vs. Trp concentration. (E) Linear plot of Log (1/ [L]) vs. Log (I_{DNA}–L/ (I_{DNA} – I_{DNA-L})) to obtain the value of the binding constant of the interaction of Trp with aptamer.

Table 1
Comparison of the analytical performance between the proposed aptasensor and other detection methods for Trp.

Sensing surface	Method	LR	LOD	Ref.
GNP/CILE	SWV	5 to 900 mM	4 mM	[30]
poly(*p*-ABSA) film/ GCE	LSV	1.0×10^{-7} - 10^{-5} M	7.0×10^{-8} M	[31]
SiO_2 nanoparticles/CPE	LSV	1.0×10^{-7}–5.0×10^{-5}M	3.6×10^{-8} M	[32]
CuCoHCF/ graphite electrode	Amperometry	10 - 900 μM	6μM	[33]
SWNT/GCE	DPV	4×10^{-8} - 1×10^{-5} M	1×10^{-8} M	[34]
PGE / GND	CV	1.0×10^{-8} -4.0×10^{-6}M	3 nM	[35]
MWCNTs/SGE	DPV	0.2×10^{-6} - 15×10^{-6}M	0.139×10^{-6} M	[36]
OPPy/CPE	ASV	10-100 mM	10 mM	[37]
–	RP-HPLC	0.25–20 μg/mL	0.0144 μg/mL	[38]
–	HPLC	–	0.46×10^{-6} M	[39]
–	HPLC	0.1–0.8 μg/mL	0.002 μg/mL	[40]
AuNPs/MWCNTs-Chit/SPE	DPV	3.0 nM- 100 μM	1 nM	This Work

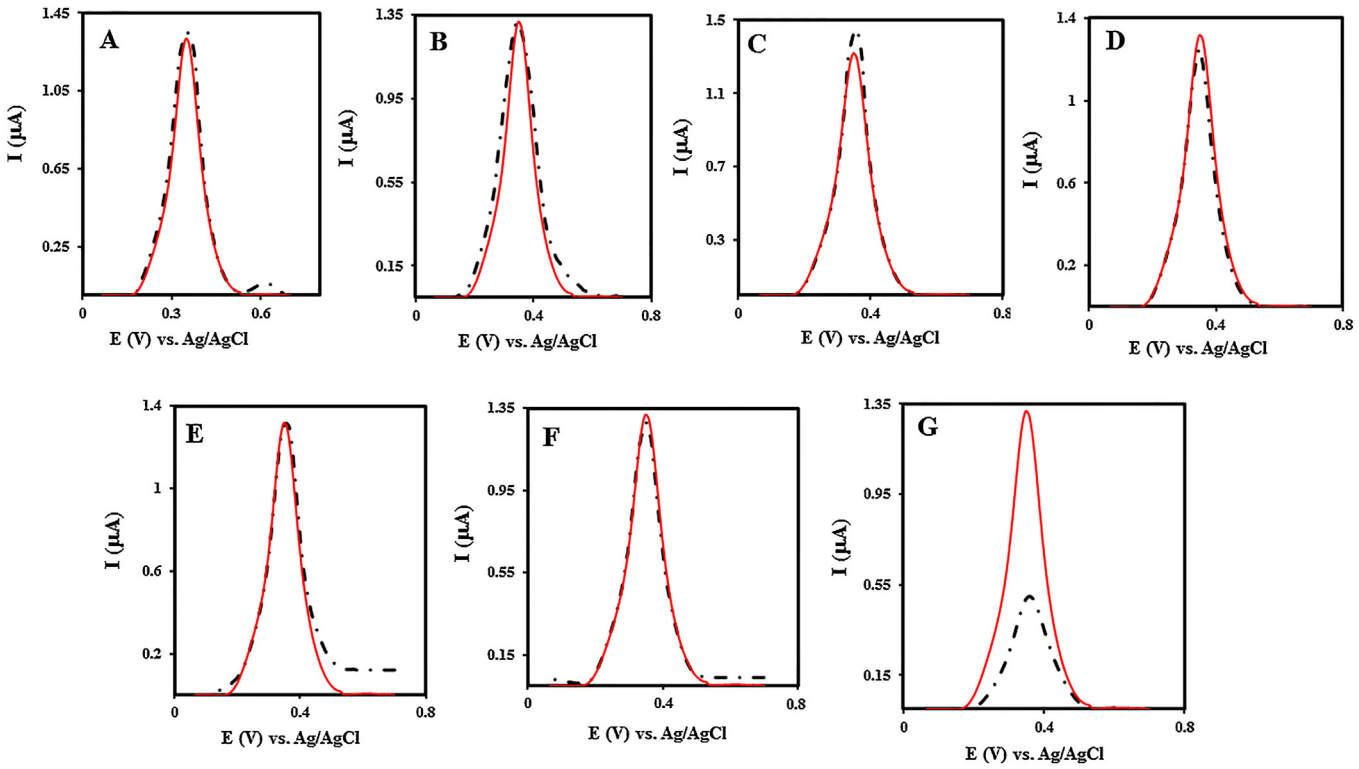

Fig. 5. Selectivity analysis for Trp detection by monitoring the DPV response of prepared aptasensor between six amino acids: A) tyrosine, B) histidine, C) arginine, D) lysine, E) valine, F) methionine and G) tryptophan. Amino acids concentration is 0.3 μM, (Dotted lines: Ind/Apt-DNA/AuNPs/MWCNTs-Chit/SPE, solid lines: amino acids/Ind/Apt-DNA/AuNPs/MWCNTs-Chit/SPE).

modified electrode surface. As seen in calibration plots (Fig. 4 B, C and D), the peak current was proportional to the concentrations of Trp over the ranges of 0.003–100 μM. The detection limit was calculated as 1.0 nM at 3σ. The comparison results of the analytical performance of this sensor with some other detection methods to determinate Trp are given in Table 1.

4.2. Binding constant

The binding constant value of the aptamer-Trp was specify according to Eq. (3) [41]:

$$\mathrm{Log}(1/[\mathrm{L}]) = \mathrm{log}K_b + \mathrm{Log}(I_{DNA}-L/(I_{DNA}-I_{DNA-L})) \quad (3)$$

Where L is the free ligand (Trp), K_b is the binding constant, I_{DNA} is the peak current of Ind on the surface of immobilized aptamer and I_{DNA-L} is the peak current of Ind on the surface of Trp/Apt-DNA/AuNPs/MWCNTs-Chit/SPE. As shown in Fig. 4E, plotting the Log (1/ [L]) versus Log (I_{DNA}–L/ (I_{DNA} – I_{DNA-L})) produces a straight line with the intercept of log K_b. The K_b of Apt-Trp complex has been obtained equal to 9×10^7 M.

4.3. Application of the aptasensor for detection of the Trp in human serum

2 In order to examine the applicability of the fabricated sensor for the determination of Trp in real samples, it was measured in the diluted healthy human serum sample (serum sample was diluted 3-folds using PBS (0.1 M, pH 7.4)). Recovery experiments were performed by adding standard solutions of Trp to the serum sample and employing them in the electrochemical experiments. As shown in Table S1, the fabricated aptasensor worked accurately for the detection of Trp in the serum samples.

Also, under the same condition, the interference effects of some amino acids were investigated on the detection of Trp in the serum sample. Recovery experiments were performed by adding several types of amino acids (tyrosine, histidine, arginine, valine and methionine) to the serum sample containing of Trp. As shown in Table S2, the aptasensor but did not show any interference effect.

4.4. Selectivity, stability and reproducibility of the Trp aptasensor

The detection specificity of the aptasensor is one of the potential advantages of an aptasensor. To prove the selectivity of the aptasensor, control experiments were performed using six amino acids: tyrosine, histidine, arginine, lysine, valine, methionine and tryptophan. As shown in Fig. 5, the decrease of $[Fe(bpy)_3](p\text{-}CH_3C_6H_4SO_2)_2$ peak current for the complex of Trp -Apt is most obvious in comparison with other mentioned amino acids at the equal concentration (0.3 μM). The obtained results demonstrate that non-specific interactions of fabricated aptasensor with other examined amino acids are almost inconsiderable.

Also, the stability of the fabricated aptasensor was examined by storing the aptasensor in PBS (pH 7.4) at 4 °C for 22 days. After this time, no remarkable change in current response was observed for the detection of Trp at the same concentration (it retained 95% of its initial response), indicating an acceptable stability of the fabricated Trp aptasensor.

The reproducibility of this method for the detection of 0.3 μM Trp was investigated on a series of five prepared aptasensors at the same experimental condition. The RSD of 2.1% has been achieved from these experiments, which indicated a satisfactory reproducibility for the prepared Trp aptasensor.

5. Conclusion

In this study, we have demonstrated a simple and reusable aptasensor for detection of an amino acid target, tryptophan, by using $[Fe(bpy)_3](p\text{-}CH_3C_6H_4SO_2)_2$ as an effective electroactive indicator. In this work, the Trp sensor was prepared by, first, modification the electrode with AuNPs/MWCNTs-Chit, which amplified

the electrochemical signals. Then the thiolated partly complementary DNA was self-assembled on the surface of modified electrode. Next, aptamer was immobilized on the prepared electrode through DNA hybridization reaction.

This is the first report of designing a reusable electrochemical Trp aptasensor using AuNPs/MWCNTs-Chit/SPE and $[Fe(bpy)_3](p\text{-}CH_3C_6H_4SO_2)_2$ together. The sensor performance was investigated by DPV, CV and EIS techniques. The incubation of the Trp by the aptamer caused the conformational change of the aptamer, formation of Trp/aptamer complex and dissociation of the Trp/aptamer complex from the electrode surface. The peak current of the $[Fe(bpy)_3](p\text{-}CH_3C_6H_4SO_2)_2$ linearly decreased by the addition of the trp concentration over the range of 0.003 to 100 μM with a detection limit as low as 1.0 nM. In addition, this aptasensor showed high selectivity for Trp in compared to other amino acids such as tyrosine, histidine, arginine, lysine, valine and methionine. Also, the proposed aptasensor was successfully used to Trp detection in human serum sample.

Appendix A. Supplementary data

Supplementary data associated with this article can be found, in the online version, at https://doi.org/10.1016/j.jpba.2018.10.006.

References

[1] J.M. Silván, J. van de Lagemaat, A. Olano, M.D. del Castillo, Analysis and biological properties of amino acid derivates formed by Maillard reaction in foods, J. Pharm. Biomed. Anal. 41 (2006) 1543–1551.
[2] H. Ali, R. Pätzold, H. Brückner, Determination of L-and D-amino acids in smokeless tobacco products and tobacco, Food Chem. 99 (2006) 803–812.
[3] A.A. Ensafi, R. Hajian, Determination of tryptophan and histidine by adsorptive cathodic stripping voltammetry using H-point standard addition method, Anal. Chim. Acta 580 (2006) 236–243.
[4] S. Striano, D. Grossi, S. Guardascione, Possible Correlations Between Sleeping Troubles and Visual Hallucinations in Patients With Parkinsons-disease on L-dopa Therapy-polygraphic Findings of a Case and Effects of L-tryptophan, Electroencephalography and Clinical Neurophysiology, Elsevier Sci Ireland Ltd Customer Relations Manager, Bay 15, Shannon Industrial Estate Co, CLARE, IRELAND, 1980, pp. P17–P18.
[5] A.-E. Radi, J.L. Acero Sánchez, E. Baldrich, C.K. O'Sullivan, Reagentless, reusable, ultrasensitive electrochemical molecular beacon aptasensor, J. Am. Chem. Soc. 128 (2006) 117–124.
[6] A.B. Hashkavayi, J.B. Raoof, Design an aptasensor based on structure-switching aptamer on dendritic gold nanostructures/Fe3O4@ SiO2/DABCO modified screen printed electrode for highly selective detection of epirubicin, Biosens. Bioelectron. 91 (2017) 650–657.
[7] L. Kashefi-Kheyrabadi, M.A. Mehrgardi, Design and construction of a label free aptasensor for electrochemical detection of sodium diclofenac, Biosens. Bioelectron. 33 (2012) 184–189.
[8] P. Miao, Y. Tang, B. Wang, K. Han, X. Chen, H. Sun, An aptasensor for detection of potassium ions based on RecJ f exonuclease mediated signal amplification, Analyst 139 (2014) 5695–5699.
[9] H. Gu, Y. Yang, F. Chen, T. Liu, J. Jin, Y. Pan, P. Miao, Electrochemical detection of arsenic contamination based on hybridization chain reaction and RecJf exonuclease-mediated amplification, Chem. Eng. J. 353 (2018) 305–310.
[10] A.B. Hashkavayi, J.B. Raoof, R. Ojani, S. Kavoosian, Ultrasensitive electrochemical aptasensor based on sandwich architecture for selective label-free detection of colorectal cancer (CT26) cells, Biosens. Bioelectron. 92 (2017) 630–637.
[11] A. Bagheri Hashkavayi, J. Bakhsh Raoof, R. Ojani, E. Hamidi Asl, Label-free electrochemical aptasensor for determination of chloramphenicol based on gold nanocubes-modified screen-printed gold electrode, Electroanalysis 27 (2015) 1449–1456.
[12] V. Pavlov, Y. Xiao, B. Shlyahovsky, I. Willner, Aptamer-functionalized Au nanoparticles for the amplified optical detection of thrombin, J. Am. Chem. Soc. 126 (2004) 11768–11769.
[13] A.B. Hashkavayi, J.B. Raoof, R. Azimi, R. Ojani, Label-free and sensitive aptasensor based on dendritic gold nanostructures on functionalized SBA-15 for determination of chloramphenicol, Anal. Bioanal. Chem. 408 (2016) 2557–2565.
[14] Z. Bagheryan, J.-B. Raoof, M. Golabi, A.P. Turner, V. Beni, Diazonium-based impedimetric aptasensor for the rapid label-free detection of Salmonella typhimurium in food sample, Biosens. Bioelectron. 80 (2016) 566–573.
[15] S.-J. Chen, C.-C. Huang, H.-T. Chang, Enrichment and fluorescence enhancement of adenosine using aptamer–gold nanoparticles, PDGF aptamer, and Oligreen, Talanta 81 (2010) 493–498.
[16] L. Fang, Z. Lü, H. Wei, E. Wang, A electrochemiluminescence aptasensor for detection of thrombin incorporating the capture aptamer labeled with gold nanoparticles immobilized onto the thio-silanized ITO electrode, Anal. Chim. Acta 628 (2008) 80–86.
[17] J. Liu, D. Mazumdar, Y. Lu, A simple and sensitive "dipstick" test in serum based on lateral flow separation of aptamer-linked nanostructures, Angew. Chem. 118 (2006) 8123–8127.
[18] S. Li, L. Xu, M. Sun, X. Wu, L. Liu, H. Kuang, C. Xu, Hybrid nanoparticle pyramids for intracellular dual MicroRNAs biosensing and bioimaging, Adv. Mater. 29 (2017) 1606086.
[19] R. Gao, C. Hao, L. Xu, C. Xu, H. Kuang, Spiny Nanorod and upconversion nanoparticle satellite assemblies for ultrasensitive detection of messenger RNA in living cells, Anal. Chem. 90 (2018) 5414–5421.
[20] W. Ma, M. Sun, P. Fu, S. Li, L. Xu, H. Kuang, C. Xu, A chiral-nanoassemblies-enabled strategy for simultaneously profiling surface glycoprotein and MicroRNA in living cells, Adv. Mater. 29 (2017) 1703410.
[21] L. Fotouhi, A.B. Hashkavayi, M.M. Heravi, Electrochemical behaviour and voltammetric determination of sulphadiazine using a multi-walled carbon nanotube composite film-glassy carbon electrode, J. Exp. Nanosci. 8 (2013) 947–956.
[22] L. Fotouhi, A.B. Hashkavayi, M.M. Heravi, Interaction of sulfadiazine with DNA on a MWCNT modified glassy carbon electrode: determination of DNA, Int. J. Biol. Macromol. 53 (2013) 101–106.
[23] F. Chekin, J.B. Raoof, S. Bagheri, S.B.A. Hamid, Fabrication of chitosan-multiwall carbon nanotube nanocomposite containing ferri/ferrocyanide: application for simultaneous detection of D-penicillamine and tryptophan, J. Chin. Chem. Soc. 59 (2012) 1461–1467.
[24] P. Pakravan, S. Kashanian, M.M. Khodaei, F.J. Harding, Biochemical and pharmacological characterization of isatin and its derivatives: from structure to activity, Pharmacol. Rep. 65 (2013) 313–335.
[25] B. Li, Y. Du, H. Wei, S. Dong, Reusable, label-free electrochemical aptasensor for sensitive detection of small molecules, Chem. Commun. (2007) 3780–3782.
[26] X. Yang, T. Bing, H. Mei, C. Fang, Z. Cao, D. Shangguan, Characterization and application of a DNA aptamer binding to L-tryptophan, Analyst 136 (2011) 577–585.
[27] S. Kianipour, A. Asghari, Room temperature ionic liquid/multiwalled carbon nanotube/chitosan-modified glassy carbon electrode as a sensor for simultaneous determination of ascorbic acid, uric acid, acetaminophen, and mefenamic acid, IEEE Sens. J. 13 (2013) 2690–2698.
[28] L. Kashefi-Kheyrabadi, M.A. Mehrgardi, E. Wiechec, A.P.F. Turner, A. Tiwari, Ultrasensitive detection of human liver hepatocellular carcinoma cells using a label-free aptasensor, Anal. Chem. 86 (2014) 4956–4960.
[29] A. Bard, L. Faulkner, J. Leddy, C. Zoski, Electrochemical Methods: Fundamentals and Applications, vol. 2, Wiley, New York, 1980.
[30] A. Safavi, S. Momeni, Electrocatalytic oxidation of tryptophan at gold nanoparticle-modified carbon ionic liquid electrode, Electroanalysis 22 (2010) 2848–2855.
[31] Y. Ya, D. Luo, G. Zhan, C. Li, Electrochemical investigation of tryptophan at a poly (p-aminobenzene sulfonic acid) film modified glassy carbon electrode, Bull. Korean Chem. Soc. 29 (2008) 928.
[32] M. Xu, M. Ma, Y. Ma, Electrochemical determination of tryptophan based on silicon dioxide nanopartilces modified carbon paste electrode, Russ. J. Electrochem. 48 (2012) 489–494.
[33] Y. Liu, L. Xu, Electrochemical sensor for tryptophan determination based on copper-cobalt hexacyanoferrate film modified graphite electrode, Sensors 7 (2007) 2446–2457.
[34] W. Huang, G. Mai, Y. Liu, C. Yang, W. Qua, Voltammetric determination of tryptophan at a single-wall carbon nanotubes modified electrode, J. Nanosci. Nanotechnol. 4 (2004) 423–427.
[35] S. Shahrokhian, M. Bayat, Voltammetric Determination of Tryptophan and 5-Hydroxytryptophan Using Graphite Electrode Modified With a Thin Film of Graphite/Diamond Nano-mixture and Determination of Omeprazole Using Graphite Electrode, Chemistry, Sharif University of Technology, 2010.
[36] M.R. Majidi, A. Salimi, E. Alipour, Development of voltammetric sensor for determination of tryptophan using MWCNTs-modified Sol-gel electrode, J. Chin. Chem. Soc. 60 (2013) 1473–1478.
[37] Z. Chen, K. Okamura, M. Hanaki, T. Nagaoka, Selective determination of tryptophan by using a carbon paste electrode modified with an overoxidized polypyrrole film, Anal. Sci. 18 (2002) 417–421.
[38] N. Sultana, M.S. Arayne, M.M. Khan, D.M. Saleem, A.Z. Mirza, Determination of tryptophan in raw materials, rat brain and human plasma by RP-HPLC technique, J. Chromatogr. Sci. 50 (2012) 531–537.
[39] C. Delgado-Andrade, J.A. Rufián-Henares, S. Jiménez-Pérez, F.J. Morales, Tryptophan determination in milk-based ingredients and dried sport supplements by liquid chromatography with fluorescence detection, Food Chem. 98 (2006) 580–585.
[40] S.A. Çevikkalp, G.B. Löker, M. Yaman, B. Amoutzopoulos, A simplified HPLC method for determination of tryptophan in some cereals and legumes, Food Chem. 193 (2016) 26–29.
[41] M.Y. Elahi, S.Z. Bathaie, M.F. Mousavi, R. Hoshyar, S. Ghasemi, A new DNA-nanobiosensor based on G-quadruplex immobilized on carbon nanotubes modified glassy carbon electrode, Electrochim. Acta 82 (2012) 143–151.